Cell. Mol. Life Sci. (2011) 68:4079–4090
DOI 10.1007/s00018-011-0694-6

Cellular and Molecular Life Sciences

RESEARCH ARTICLE

LAPTM4A interacts with *hOCT2* and regulates its endocytotic recruitment

A. Grabner · S. Brast · S. Sucic · S. Bierer · B. Hirsch · H. Pavenstädt · H. H. Sitte · E. Schlatter · G. Ciarimboli

Received: 16 November 2010 / Revised: 5 April 2011 / Accepted: 19 April 2011 / Published online: 8 May 2011

Abstract Human organic cation transporter 2 (*hOCT2*) is involved in the transport of endogenous and exogenous organic cations mainly in cells of the kidney and the brain. Here, we focus on the regulation of *hOCT2* by direct protein–protein interaction. Screening within a mating-based split-ubiquitin-yeast-two-hybrid system (mBSUS) revealed the lysosomal-associated protein transmembrane 4 alpha (*LAPTM4A*) as a potential interacting protein. Interaction of *LAPTM4A* and *hOCT2* was confirmed by pulldown assays, FRET microscopy analysis and immunofluorescence microscopy. Functionally, overexpression of *LAPTM4A* significantly decreased ASP^+ uptake in HEK293 cells stably transfected with *hOCT2*, suggesting a negative regulation of *hOCT2*-mediated transport. Furthermore, overexpression of *LAPTM4A* leads to a significantly decreased *hOCT2* plasma membrane expression in surface biotinylation experiments. In addition, significant expression of *LAPTM4A* in human kidney was demonstrated by immunoblotting and immunofluorescence.

In this work, *LAPTM4A* has been identified as interaction partner of *hOCT2*. *LAPTM4A* regulates the function of *hOCT2* by influencing its trafficking to/from the cell membrane and processing it via the intracellular sorting machinery.

Keywords Organic cation transporter · *LAPTM4A* · Trafficking · Regulation · Endocytosis

Introduction

Organic cations (OC) are substances of endogenous or exogenous origin that are positively charged at physiological pH. Among several different transport systems, especially organic cation transporters (OCTs) play a crucial role in transport of OCs across plasma membranes. Since endogenous substances like dopamine [1], histamine [2], and creatinine [3] as well as exogenous compounds like many drugs (for example, the histamine receptor antagonist cimetidine [4], the oral antidiabetic metformin [5] and the antineoplastic drug cisplatin [6, 7], are substrates for OCTs, these transporters exhibit important physiological, pharmacological and toxicological implications.

The transport mediated by OCTs is electrogenic, Na^+ and pH independent, bidirectional and polyspecific [8, 9]. As members of the solute carrier family 22 (SLC22A), organic cation transporters exhibit typical common characteristics like 12 transmembrane domains (TMDs), intracellular C- and N-termini, a large extracellular loop between TMDs 1 and 2 with several glycosylation sites as well as a large intracellular loop with potential phosphorylation sites between TMDs 6 and 7 [10].

Three isoforms of OCTs (OCT1-SLC22A1, OCT2-SLC22A2, OCT3-SLC22A3) have been identified. They are expressed in a species- and isoform-specific manner mainly in epithelia but also in neuronal tissue [11].

A. Grabner and S. Brast contributed equally to this work.

A. Grabner (✉) · S. Brast · B. Hirsch · H. Pavenstädt · E. Schlatter · G. Ciarimboli
Medizinische Klinik und Poliklinik D, Abteilung für Experimentelle Nephrologie, Universitätsklinikum Münster, Domagkstrasse 3A, 48149 Münster, Germany
e-mail: alexander.grabner@ukmuenster.de

S. Sucic · H. H. Sitte
Center for Physiology and Pharmacology, Institute of Pharmacology, Medical University Vienna, Vienna, Austria

S. Bierer
Klinik und Poliklinik für Urologie, Universitätsklinikum Münster, Münster, Germany

In this work, we focus mainly on human OCT2 (*hOCT2*). *hOCT2* was found to be preferentially expressed in the human body in two regions: in dopaminergic brain regions [12] and in the kidney [13]. In the brain, *hOCT2* shows the highest expression in the substantia nigra pars compacta, the area with the highest density of dopamine cell bodies in the central nervous system (CNS) [12]. Here, *hOCT2* seems to play a decisive role in the regulation of the interplay between the endogenous neuromodulators of the central dopaminergic transmission cyclo(his-pro) and salsolinol, a function that is crucial for nigral cell integrity and detoxification [12]. In human kidney, *hOCT2* is exclusively localized in the basolateral membrane of proximal tubule cells [14], where it plays an important role in the elimination of metabolites and especially of xenobiotics, being in this way a fundamental system determining systemic exposition to drugs. To cope with these dynamic challenging functions, a tight regulation of transport activity is required.

OCT expression, as an example for long-term regulation, is under developmental as well as hormonal control, at least in animal models. For example, testosterone significantly determines expression and leads to much higher levels of *rOCT2* in male than in female rats [15]. This effect seems to be mediated by stimulation of androgen responsive stimulated promoter activity [16]. Rapid regulation of OCTs can be mediated by several kinases in an isoform-specific fashion [17–21], whereas the regulation via calmodulin (CaM) is conserved through the OCT family but gender dependent [22].

Hitheto, little has been known about interaction of OCTs with other cellular proteins. Such an interaction is of great importance for the cellular processing of the transporter and, in this way, for regulation of its activity. Therefore, the aims of the present study were to identify interaction partners of *hOCT2* and to elucidate their eventual role in the regulation of *hOCT2*. Potential interaction partners were identified by means of a mating-based split-ubiquitin system (mbSUS) screening, confirmed with pulldown experiments and FRET analysis and the functional relevance was investigated with microfluorimetric uptake measurements.

Materials and methods

DNA constructs

The full-length human organic cation transporter 2 (SLC22A2, NM 003058) cloned in the expression vector pRc/CMV was kindly provided by H. Koepsell (University of Würzburg).

For expression analysis, the vector pcDNA6.F9 was kindly provided by T. Weide (University of Münster). Control transfections included the vector pcDNA 3.1 (Invitrogen, Karlsruhe, Germany). The following fluorescent vectors (Clontech, Heidelberg, Germany) were used for microscopy and FRET: pEGFP-N3, pDsRed2-N1, pEYFP-N1, pECFP-N1 and pECFP-C1.

Oligonucleotides (MWG, Ebersberg, Germany) for amplification, cloning and RT-PCR are listed in Table 1.

Mating-based split-ubiquitin system

The *hOCT2* cDNA was subcloned into the pMETYCgate vector [38], expressed in the reporter yeast strain THY.AP5 and expression was verified in western blot analysis (data not shown). Yeast cells expressing *hOCT2* were cotransformed with a human cDNA kidney library expressed in the vector pPR3-N (Dualsystems Biotech, Schlieren, Switzerland). Selection of positive interactions was performed in single dropout media lacking tryptophan and leucine. Plasmid DNAs were isolated with Zymoprep Yeast Plasmid Miniprep Kit (Zymoresearch, Freiburg, Germany), retransformed in *E.coli* XL-1-Blue, reisolated with Zyppy Plasmid Miniprpep Kit (Zymoresearch) and verified by automated sequencing (screen for primer: 5′-GTC GAA AAT TCA AGA CAA GG-3′). The same procedure was used with *hOCT1* and *hOCT3* cDNA. Furthermore, interaction was verified by yeast mating assays between THY.AP4 and THY.AP5 yeast strains expressing Cub and Nub fusion proteins including positive (Nub WTX and Cub *hOCT2*) and negative controls (empty Nub and Cub *hOCT2*).

Pulldown assay and western blot analysis

For pulldown experiments, *LAPTM4A* was cloned into the vector pcDNA6.F9 containing a FLAG and 6xHIS-Tag and expressed in HEK293 cells. Cells, transiently transfected with *LAPTM4A* (HEK293-*LAPTM4A* cells), were washed with ice-cold phosphate buffered saline (PBS) and scraped with 1 ml lysis buffer (containing Triton X-100 1% (v/v), glycerin 30% (v/v), a complete proteinase inhibitor cocktail (1 mini-pill to 10 ml; Roche, Mannheim, Germany), and in mM: 150 NaCl, 50 Tris pH 7,4, 1 EDTA, 1 EGTA, 10 $NaVO_3$). Thereon cells were sonicated for 30 s, agitated on a rotating rocker at 4° C for 30 min, and centrifuged at 700*g* for 10 min at 4° C to remove insoluble cellular debris. *LAPTM4A* lysates were then linked to Talon Sepharose beads (Clontech) and incubated with total membrane fractions of HEK293 cells stably expressing *hOCT2* (HEK293-*hOCT2*) for 2 h at 4° C. To obtain total membrane fractions, confluent cell monolayers of HEK293 cells stably expressing *hOCT2* (kindly provided by H. Koepsell, University of Würzburg) were rinsed with ice-cold PBS and then scraped in 1 ml of PBS. Crude

Table 1 Sequences of primers used for amplification (*a*), cloning (*b*) and RT-PCR (*c*)

a) Oligonucleotides for amplification and cloning	
For-LAPTM4A	5′-GAA TCC ACG CGT ATG GTG TCC ATG AGT TTC AAG-3′
Rev-LAPTM4A	5′-AC TCG AGC GGC CGC TCA GGC AGG TAA GTA AGG AG-3′
For-LAPTM4A-FRET	5′-GAG CTC AAG CTT GAA TTC ATG GTG TCC ATG AGT TTC AAG-3′
Rev-LAPTM4A-FRET	5′-TGG ATC CCG GGC GGC GGC CGC GGC AGG TAA GTA AGG AGG TG-3′
For-LAPTM4A-CFP	5′-CGA GCT CAA GCT TCG ATG GTG TCC ATG AGT TTC AAG-3′
Rev-LAPTM4A-CFP	5′-TGG ATC CCG GGC GGC GGC CGC GGC AGG TAA GTA AGG AGG TG-3′
For-hOCT2-GFP	5′-CTC AGA TCT CGA GCT ATG CCC ACC ACC GTG GAC GAT-3′
Rev-hOCT2-GFP	5′-CGG GAT GGA TCC GTT CAA TGG AAT GTC TAG TTT-3′
For-hOCT2-DsRed	5′-TCA GAT CTC GAG ATG CCC ACC ACC GTG GAC GAT-3′
Rev-hOCT2-DsRed	5′-CGG TGG ATC CCG GGC GTT CAA TGG AAT GTC TAG TTT-3′
b) Oligonucleotides for mBSUS in vivo cloning	
For-hOCT1-B1	5′-ACA AGT TTG TAC AAA AAA GCA GGC TCT CCA ACC ACC ATG ATG CCC ACC GTG GAT GAC ATT-3′
Rev-hOCT1-B2	5′-TCC GCC ACC ACC AAC CAC TTT GTA CAA GAA AGC TGG GTA GGT GCC CGA GGG TTC TGA GGT-3′
For-hOCT2-B1	5′-ACA AGT TTG TAC AAA AAA GCA GGC TCT CCA ACC ACC ATG ATG CCC ACC ACC GTG GAC GAT-3′
Rev-hOCT2-B2	5′-TCC GCC ACC ACC AAC CAC TTT GTA CAA GAA AGC TGG GTA GTT CAA TGG AAT GTC TAG TTT-3′
For-hOCT3-B1	5′-ACA AGT TTG TAC AAA AAA GCA GGC TCT CCA ACC ACC ATG ATG CCC TCC TTC GAC GAG GCG-3′
Rev-hOCT3-B2	5′-TCC GCC ACC ACC AAC CAC TTT GTA CAA GAA AGC TGG GTA AAG GTG AGA GCG GGA AAC TGG-3′
c) Oligonucleotides for RT-PCR	
For-LAPTM4A	5′-GCG GAA CCG CAG TGA CCG GTT-3′
Rev-LAPTM4A	5′-GAT GAG TCA CTT CCA CAG TCA GC-3′
For-hOCT2	5′-CAT TGA ACT AAG AAG AGA GAC CG-3′
Rev-hOCT2	5′-CCA CAG TGT ACA ATA GAC TCC A-3′
For-GAPDH	5′-CAA GCT CAT TTC CTG GTA TGA C-3′
Rev-GAPDH	5′-GTG TGG TGG GGG ACT GAG TGT GG-3′

membranes were isolated with plasma membrane protein extraction kit, according to the protocol of the manufacturer (Membrane Protein Extraction Kit; Biovision, Mountain View, USA).

After washing two times with 1 ml washing buffer (containing in mM: 50 Na_3PO_4, 30 NaCl), proteins were eluted by centrifugation at 650*g* for 3 min with 50 µl elution buffer (containing in mM: 50 Na_3PO_4, 30 NaCl, 150 imidazole).

In the case of human kidney, small parts of biopsy samples were lysed in 100 µl lysis buffer, crushed and heated at 99°C for 5 min. Lysates were then obtained by centrifugation at 13,000*g* for 10 min. After heating at 99°C for 10 min, proteins were resolved on SDS-PAGE and transferred to polyvinylidene fluoride (PVDF) membranes for western blot analysis. Immunoblotting was performed with anti-*rOCT2* antibody (Alpha Diagnostics, San Antonio, USA), anti HIS antibody (R&D Systems, Wiesbaden, Germany) and anti-*LAPTM4A* antibody (Santa Cruz, Heidelberg, Germany). Immunoreactive bands were detected with horseradish peroxidase (HRP)-conjugated secondary antibodies (Dako, Hamburg, Germany) and enhanced chemiluminescence.

Surface biotinylation experiments

For analyzing quantitative *hOCT2* surface expression, *hOCT2* stably transfected HEK293 cell monolayers were transiently transfected with either *LAPTM4A* or the empty vector pcDNA3.1 as described above. After 24 h surface proteins were biotin labeled, quenched, lysed, sonicated, and clarified by centrifugation according to the manufacturer's protocol (Membrane Protein Extraction Kit; Biovision). To isolate biotin-labeled proteins, lysates were incubated with immobilized NeutrAvidin TM Gel, washed and then incubated 1 h with SDS-PAGE sample buffer, including 50 mM dithiothreitol (DTT). Eluates were analyzed for *hOCT2* by immunoblotting.

Fluorescence resonance energy transfer

FRET signals were measured with an epifluorescence microscope (Carl Zeiss Axiovert 200) using the "three-filter method" according to Xia and Liu [39]. HEK293 cells were seeded onto poly-D-lysine-coated glass coverslips (24 mm diameter). The next day, cells were

transiently transfected with different constructs using the calcium phosphate precipitation method: 1–3 μg of cDNA was mixed with $CaCl_2$ and HBS buffer (in mM: 280 NaCl, 10 KCl, 1.5 Na_2HPO_4, 12 dextrose, 50 HEPES); after 6–10 min, the calcium phosphate–DNA precipitate was added to the cells. After 4–5 h, the cells were washed twice with PBS and briefly treated with glycerol, followed by the addition of fetal calf serum-containing medium. Medium was replaced by Krebs-HBS buffer (in mM: 10 HEPES, 120 NaCl, 3 KCl, 2 $CaCl_2$, 2 $MgCl_2$) and images were taken using a ×63 oil objective and a LUDL filter wheel that allows for rapid exchange of filters. The system was equipped with the following fluorescence filters: CFP filter (ICFP; excitation = 436 nm, dichroism = 455 nm, emission = 480 nm), YFP filter (IYFP; excitation = 500 nm, dichroism = 515 nm, emission = 535 nm), and FRET filter (IFRET; excitation = 436 nm, dichroism = 455 nm, emission = 535 nm). The acquisition of the images was done with MetaMorph version 4.6. (Molecular Devices, Downingtown, PA, USA). Background fluorescence was subtracted from all images, and fluorescence intensity was measured at the plasma membrane and in cytosolic regions in all images. To calculate a normalized FRET signal (NFRET), we used the following equation:

$$N_{FRET} = \frac{I_{FRET} - a \times I_{YFP} - b \times I_{CFP}}{\sqrt{I_{YFP} \times I_{CFP}}}$$

where a and b represent the bleed-through values for YFP and CFP. All NFRET values are expressed as mean ± SEM. Corrected FRET (FRETc) images were obtained according to [40]. Briefly, after background subtraction from all three images, CFP and YFP images were multiplied with their corresponding bleed-through value. The following equation was used for the calculation of FRETc images, FRETc = FRET − (b × CFP) − (a × YFP). FRET signals were calculated and displayed with ImageJ PixFRET software [41] (downloadable at http://rsb.info.nih.gov/ij/).

Positive control experiments included either expression of the tandem CFP-YFP or co-expression of CFP-serotonin transporter (*SERT*) and YFP-*SERT*. *SERT* has been shown to homo-oligomerize by FRET microscopy and biochemical approaches [42]. Negative control experiments included coexpression of CFP and YFP or the coexpression of *hOCT2*-CFP and Pal-Myr-YFP, a YFP construct with a signal sequence tethering the YFP-moiety to the plasma membrane.

Microdissection of human proximal tubules

Human proximal tubules were obtained from patients undergoing tumor nephrectomy. Pieces of normal kidney tissue surrounding the tumor were used. The procedure was approved by the ethics commission of the Universitätsklinikum Münster, and written consent was obtained from each patient. Renal tissue was transferred into chilled HCO_3-free phosphate buffer immediately after nephrectomy. Parts of the renal tissue were cut into small pieces (≈5–7 mm^3 each), and tubules were enzymatically isolated according to our method previously published [43]. Selected tubules of a total length of approximately 40 mm were lysed in a 4-M guanidinium chloride buffer, and total RNA was isolated using the RNeasy-kit (Qiagen, Hilden, Germany). Isolated total RNA was incubated with 10 U of DNase I (Promega, Heidelberg, Germany) at 37°C for 1 h to digest isolated traces of genomic DNA. RNA was separated using a RNeasy column (Qiagen) and cDNA first strand synthesized using Moloney murine leukemia virus-reverse transcriptase (Promega).

Immunostaining

hOCT2-GFP stably expressing cells seeded on glas cover slips were transiently transfected with FLAG-*LAPTM4A*. After 48 h, cells were fixed in 100% ethanol, permeabilized with 1% Triton, and blocked in PBS with 5% gelatine. Cells were stained with anti Flag antibody (Sigma, Crailsheim, Germany) to visualize *LAPTM4A*, then incubated in secondary antibodies (Alexa 594; Invitrogen). Images were acquired using an Axio Zeiss confocal microscope.

For further analysis, HEK293 cells were transiently transfected with *LAPTM4A* and *hOCT2*-YFP and colocalization studies were performed using primary antibodies against *LAPTM4A* (Sigma), EEA1 (BD, Heidelberg, Germany) and *LAMP1* (DSHB) and Star36D 488 (AbD Serotec, Düsseldorf, Germany) and Alexa 594 secondary antibodies.

The *LAMP1* antibody, developed by J.T. August and J.E.K. Hildreth, was obtained from the Developmental Studies Hybridoma Bank developed under the auspices of the NICHD and maintained by The University of Iowa, Department of Biology, Iowa City, IA 52242.

In the case of human kidneys, 5-μm-thick cryosections were blocked in PBS with 10% normal goat serum. After incubation with primary antibodies against *hOCT2* (kindly provided by H. Koepsell, University of Würzburg) and *LAPTM4A*, washing with PBS and incubation with secondary antibodies (Alexa 594 and Star36D 488, respectively) sections were rinsed with PBS, coverslipped with Crystal Mount (GeneTex, San Antonio, TX, USA) and evaluated by epifluorescence microscopy (Observer Z1 with apotome; Zeiss, Göttingen, Germany). Negative control slides were included without addition of primary antibody.

Cell culture and transfection

HEK293 cells (CRL-1573; American Type Culture Collection, Rockville, MD, USA), as wild-type (WT) and

stably expressing *hOCT2* cells, were grown at 37° C in 50-ml cell culture flasks (Greiner, Frickenhausen, Germany) in DMEM (Biochrom, Berlin, Germany) containing 3.7 g/l $NaHCO_3$, 1.0 g/l D-glucose, and 2.0 mM L-glutamine (Biochrom), and gassed with 8% CO_2. Penicillin (100 U/ml), 100 mg/l streptomycin (Biochrom), 10% fetal bovine serum, and, only for OCT-transfected cells, 0.8 mg/ml geneticin (PAA Laboratories, Coelbe, Germany) were added to the medium.

HEK293 WT and *hOCT2* expressing cells were transiently transfected with either control vector pcDNA3.1 or *LAPTM4A* using the Turbofect method, as recommended by the manufacturer (Fermentas, St. Leon-Rot, Germany).

Real-time PCR

Gene expression profiles were analyzed by real time PCR. Total RNA from HEK293 *hOCT2* expressing *LAPTM4A* transiently transfected cells were isolated using RNeasy-kit (Qiagen). For cDNA synthesis, 2 µg total RNA was used with the SuperScript-III First-Strand Synthesis SuperMix (Invitrogen). Real time PCR was performed using SYBR Green PCR Master Mix on an ABI PRISM 7700 Sequence Detection System. Specific primer pairs as listed below were used. All instruments and reagents were purchased from Applied Biosystems (Darmstadt, Germany). Relative gene expression values were evaluated with the 2-DDCt method using *GAPDH* as housekeeping gene [44].

Microfluorimetric uptake measurements

Organic cation uptake by *hOCT2*-expressing cells was measured using a fluorescent plate reader (Infinity M200; Tecan, Crailsheim, Germany), according to the method described by us previously [22]. As substrate for OCTs, the fluorescent organic cation 4-[4-(dimethylamino)styryl]-N-methylpyridinium (ASP^+) at a concentration of 1 µM was used. Cells confluently grown on 96-well microplates (Nunclon 96 Flat bottom; Nunc, Wiesbaden, Germany) were excited with monochromatic light of 450 nm and fluorescence emission, filtered by a second monochromator at 590 nm, was finally measured by a fluorescence detector at 37°C. Fluorescence was measured dynamically in each well before and after ASP^+-injection. ASP^+ uptake was quantified by linear regression of the initial (appr. 30–40 s) fluorescence increase.

Chemicals

All substances and standard chemicals were obtained from Sigma or Merck (Darmstadt, Germany), except where otherwise specified.

Statistical analysis

Data are presented as mean values ±SEM, with *n* referring to the number of monolayers used in the experiments. Unpaired two-sided Student's *t* test or ANOVA (with Turkey post-test) were used to prove statistical significance of the effects using GraphPad Prism 5.3 (GraphPad Software, San Diego, CA, USA). A *P* value <0.05 was considered statistically significant.

Results

Identification of *LAPTM4A* as an *hOCT2* interacting protein

To identify proteins that interact with *hOCT2*, a screening with the mating-based split ubiquitin yeast two-hybrid system using a human kidney library was performed. The mbSUS is a special yeast two-hybrid technique for membrane proteins, where interactions of proteins take place in vivo directly at the plasma membrane. This system allows in vivo cloning of PCR products by recombination into expression vectors, mating-based detection of the interactions, and improved selection of interacting fusions on media lacking histidine and adenine. B1–B2-linked full-length *hOCT2* cDNA was cloned in vivo in-frame into the expression vector pMETYCgate containing the C-terminal one-half of ubiquitin and the transcription factor protA-LexA-VP16 peptide. This construct was then used to screen an adult human kidney library of clones fused to the mutated form of ubiquitin in the pPR3-N vector (Dualsystems Biotech) by means of cotransformation into the THY.AP5 yeast strain. This screening resulted in 283 independent clones that induced activation of reporter genes. After sequencing, 15 clones were identified encoding full-length sequence of lysosomal-associated protein transmembrane 4 alpha (*LAPTM4A*). Interactions were confirmed in yeast mating assays (Fig. 1). False positives due to self-activation of *hOCT2* and *LAPTM4A* where excluded by cross-plating transformed yeasts on minimal media. *LAPTM4A* is an intracellularly localized membrane protein associated to lysosomes and late endosomes. This protein contains four transmembrane domains with cytoplasmic N and C termini. In addition, B1–B2-linked full-length *hOCT1* or *hOCT3* cDNA was cloned in vivo in-frame into the expression vector pMETYCgate, and their interaction with *LAPTM4A*-cDNA fused to the mutated form of ubiquitin in the pPR3-N vector was investigated. An interaction between *hOCT1*/*hOCT3* and *LAPTM4A* could also be observed (data not shown).

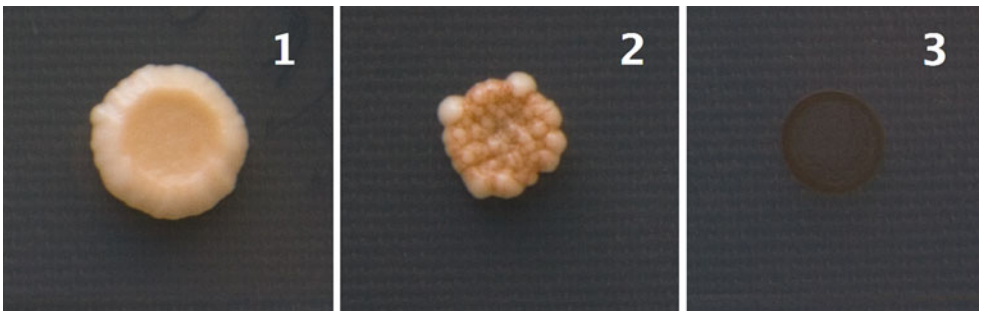

Fig. 1 Yeast mating assay demonstrates interaction between *LAPTM4A*-Nub and *hOCT2*-Cub (*1*). Nub-WTX and *hOCT2*-Cub function as positive control (*2*), whereas lack of interaction between *hOCT2*-Cub and the empty Nub vector indicates a negative control (*3*)

Pulldown assay between *LAPTM4A* and *hOCT2*

To confirm interaction in vitro in a mammalian cell context, we performed HIS-pulldown assays of *LAPTM4A* and *hOCT2* cell lysates. As shown in Fig. 2, western blot analysis of *LAPTM4A/hOCT2* eluates with polyclonal *rOCT2* antibody (Alpha diagnostics) demonstrates *hOCT2*-*LAPTM4A* protein–protein interaction, whereas *hOCT2* eluates on its own functioned as a negative control. These data validate our previous results and suggest a physical interaction between *LAPTM4A* and *hOCT2*.

Colocalization of *LAPTM4A* and *hOCT2* in lysosomes and late endosomes of HEK293 cells by immunofluorescence microscopy

To investigate where exactly *LAPTM4A* and *hOCT2* are colocalized, FLAG-*LAPTM4A* and *hOCT2*-GFP were transfected into HEK293 cells and their cellular distribution was analyzed by confocal microscopy. As a membrane bound transporter, *hOCT2* exhibits a typical predominantly membraneous staining (Fig. 3), whereas *LAPTM4A* has a punctate vesicular staining with emphasis on submembranous vesicular structures (Fig. 3). Previous studies have already described these multiple intracellular locations including mainly late endosomes and lysosomes [23]. Nevertheless, at least partial colocalization of *LAPTM4A* and *hOCT2* was found exactly in these submembranous vesicles These findings were confirmed by further colocalization experiments, where *LAPTM4A*, overexpressed in HEK293 cells, colocalizes with *LAMP1* (lysosomal-associated membrane protein 1) (Fig. 4), a marker for late endosomes and lysosomes, but not with *EEA1* (early

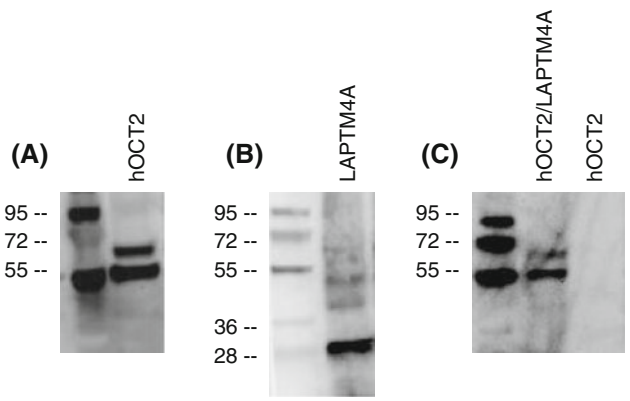

Fig. 2 *hOCT2* interacts in vitro with *LAPTM4A* in a pulldown assay. **a** Western blot analysis of HEK293-*hOCT2* cells exhibits the transporter in a glycosilated (72 kDa) and non-glycosilated (55 kDa) form. **b** Western blot analysis of HEK293-*LAPTM4A* cells. *LAPTM4A* is detected with anti-HIS antibody at 28 kDa. **c** Pulldown assay of lysates from HEK293-*LAPTM4A* cells linked to talon sepharose beads via 6× HIS tag and incubated with lysates from HEK293-*hOCT2* cells demonstrates physical interaction, whereas pulldown performed with lysates from HEK293-*hOCT2* cells alone was negative (negative control of pulldown assay)

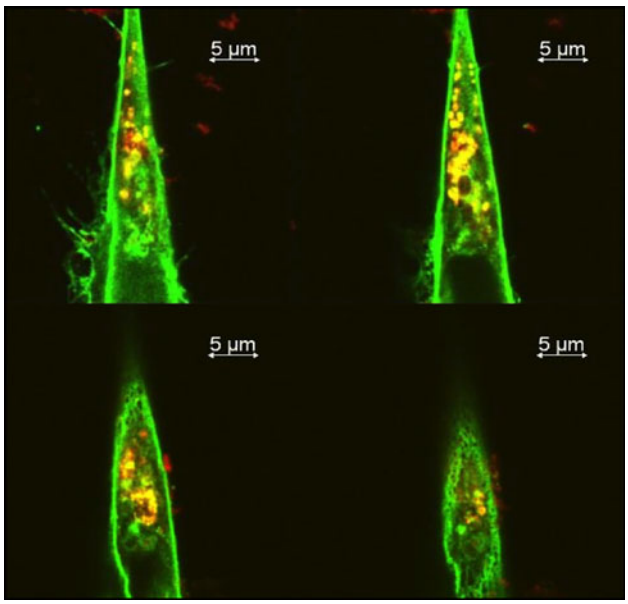

Fig. 3 HEK293 *hOCT2*-GFP-tagged stably transfected cells were transiently transfected with FLAG-tagged *LAPTM4A*. After cell fixation and staining with anti-FLAG antibody, primary antibodies were visualized with ALEXA 594 secondary antibodies. Shown are merged confocal images, where co-localization of *hOCT2*-GFP and FLAG-tagged *LAPTM4A* is observed as signals (*yellow*)

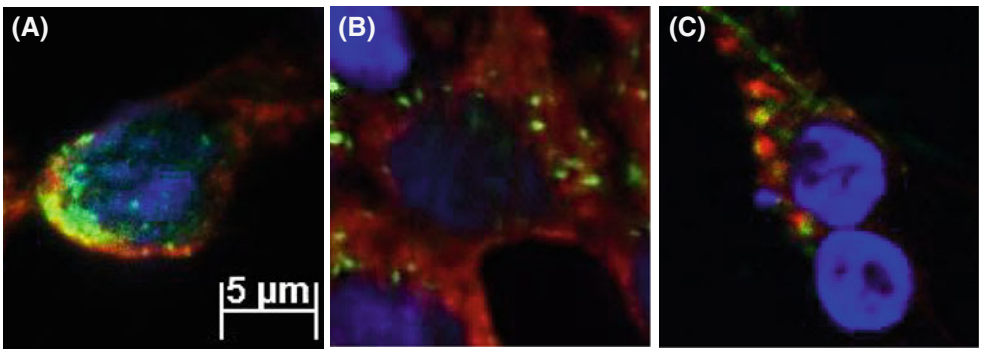

Fig. 4 HEK293 cells were transiently transfected with *LAPTM4A* (**a**, **b**) or *LAPTM4A* and *hOCT2*-YFP (**c**). After fixation, cells were stained with primary antibodies against *LAPTM4A* (**a–c**), *LAMP1* (**a**) and *EEA1* (**b**), respectively, and visualized with Alexa 594 (**a–c**) and Star36D 488 (**a**, **b**) secondary antibodies. Shown are merged images, where *LAPTM4A* (*green*) and *LAMP1* (*red*) colocalize as signals (*yellow*) (**a**). On the contrary, no significant colocalization was found between *LAPTM4A* (*green*) and *EEA1* (*red*) (**b**). After overexpression of *LAPTM4A*, *hOCT2*-YFP (*green*) colocalizes with *LAMP1* (*red*) (**c**)

endosome antigen 1), a marker for early endosomes (Fig. 4). Moreover, overexpression of *LAPTM4A* in cells, transiently transfected with *hOCT2*-YFP, leads to colocalization of the transporter with *LAMP1* (Fig. 4), thus indicating that lysosomes and late endosomes are the precise place of interaction of *LAPTM4A* and *hOCT2*.

FRET analysis of *LAPTM4A* and *hOCT2* interaction in HEK293 cells

As an additional independent approach, we used fluorescence resonance energy transfer microscopy to confirm whether the previously in vivo and also in vitro observed interaction between *LAPTM4A* and *hOCT2* occurs in living cells. For FRET measurements, HEK293 WT cells were transiently cotransfected with carboxy-CFP-tagged *LAPTM4A* (*LAPTM4A*-CFP) and amino- or carboxy-YFP-tagged *hOCT2* (YFP-*hOCT2*/*hOCT2*-YFP). Positive control experiments included transfection with CFP-YFP in tandem, as well as coexpression of carboxy-CFP and carboxy-YFP-tagged human serotonin transporter (*SERT*), which in several studies has been shown to oligomerize in the plasma membrane [24]. We observed significant FRET signals when *LAPTM4A* and *hOCT2* were coexpressed in HEK293 cells in submembraneous vesicular structures, which were selected according to our immunofluorescent findings. Measurements of these regions were performed in 10 transfected cells. As expected, FRET values were detected (mean value of 0.264 ± 0.016) between *SERT*-CFP and *SERT*-YFP. As negative controls localized within the cytosol, CFP and YFP alone were cotransfected, as well as *hOCT2*-CFP and PAL-MYR-YFP. PAL-MYR-YFP is localized exclusively to the plasma membrane, thus indicating a membrane bound negative control [25] with mean FRET signals (mean FRET values 0.081 ± 0.012), which were not significantly different from CFP plus YFP (mean FRET values 0.014 ± 0.005). In contrast, coexpression of *LAPTM4A*-CFP and YFP-*hOCT2* and *hOCT2*-YFP, respectively, exhibited mean normalized FRET values of 0.239 ± 0.013 and 0.253 ± 0.023 (Fig. 5), revealing interaction in both experiments and confirming our biochemical findings. Together with the pulldown and colocalization experiments, these results indicate that *LAPTM4A* and *hOCT2* coexist in the same cellular regions and interact.

Expression of *LAPTM4A* on mRNA levels in human proximal tubule cells

Total RNA from HEK293 WT cells as well as from freshly isolated proximal tubule cells from human biopsy samples was isolated and used for cDNA synthesis. Apart from RT-PCR experiments, PCR with *LAPTM4A* specific primers demonstrated significant expression in isolated human proximal tubules as well as in HEK293 WT cells on mRNA levels (Fig. 6).

Expression of *LAPTM4A* on protein levels in human kidney

In order to verify significant *LAPTM4A* expression lysates of biopsy samples of human kidneys were assembled and western blot analysis was performed. Using an anti-*LAPTM4A* antibody we were able to detect significant *LAPTM4A* expression on protein level in human kidney (Fig. 6).

Colocalization of *LAPTM4A* and *hOCT2* in lysosomes and late endosomes of human kidneys

LAPTM4A expression in human kidneys was further analyzed by immunofluorescence microscopy. *LAPTM4A* is

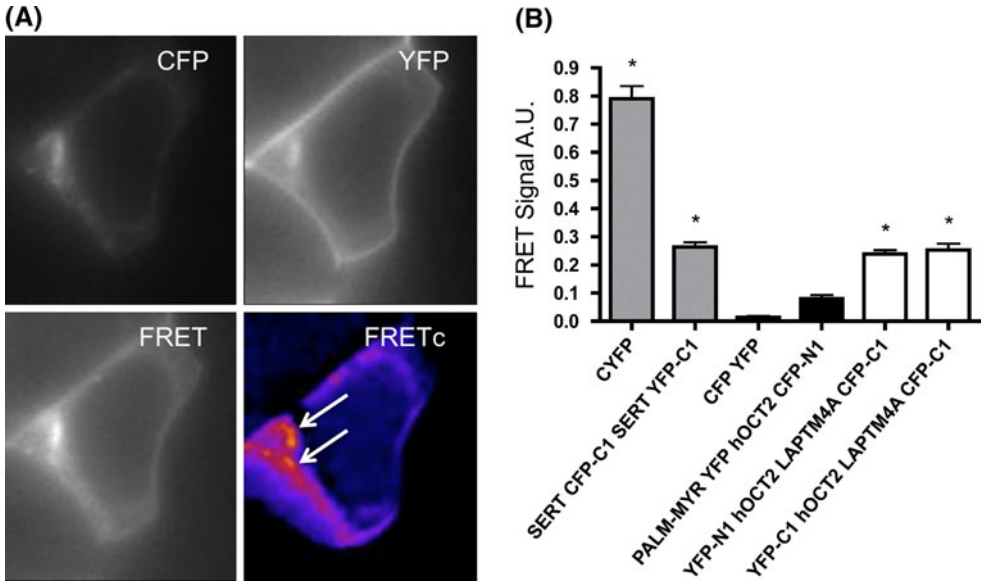

Fig. 5 Interaction between *LAPTM4A* and *hOCT2* visualized by FRET microscopy. **a** High magnification of a HEK293 cell transfected with YFP-*hOCT2* and CFP-*LAPTM4A* (*top left panel* CFP channel, *top right panel* YFP channel, *bottom left panel* FRET channel, *bottom right panel* corrected FRET channel). *arrowheads* indicate processes in which FRET was detected. FRETc images are displayed using pseudocolors with the spectrum inset representing fluorescence intensity **b** Results of FRET analysis. Positive control experiments included cells transfected with a CFP-YFP tandem construct and cells coexpressing CFP-*SERT* and YFP-*SERT*, negative controls included cells cotransfected with CFP and YFP and cells coexpressing PALM-MYR-YFP and *hOCT2*-CFP. The intensity of FRET was measured for the different combination of CFP/YFP pairs and expressed as normalized FRET values as described in "Materials and methods". Ten independent cells were analyzed for FRET measurements each. *Error bars* SEM; *Statistically significant differences from negative controls (ANOVA) ($P < 0.05$)

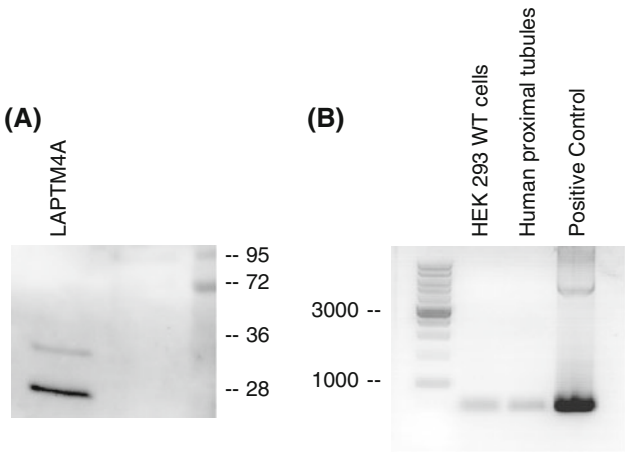

Fig. 6 Western blot analysis of human kidney biopsy samples with anti-*LAPTM4A* antibody exhibits significant *LAPTM4A* expression at 28 kDa (**a**). Furthermore, PCR with cDNA demonstrates *LAPTM4A* expression on mRNA Levels in HEK293 cells as well as human proximal tubules (**b**). (Positive control, taken from mBSUS interaction screen)

expressed in all tubular segments of the human kidney. Partial colocalization with *hOCT2*, a membrane bound transporter predominantly expressed in the basolateral membrane, was found only in submembraneous vesicular structures of proximal tubule cells (Fig. 7). Again, significant colocalization of *LAPTM4A* with *LAMP1* but not with *EEA1* revealed that lysosomes and late endosomes are the definite location of interaction (Fig. 7).

Functional interaction between *LAPTM4A* and *hOCT2*

To investigate the functional consequences of the interaction between *LAPTM4A* and *hOCT2*, microfluorimetric uptake measurements were performed. As substrate for OCTs, we used the prototypic fluorescent organic cation ASP^+ at a concentration of 1 µM. ASP^+ uptake was measured in *hOCT2* stably transfected cells (*hOCT2* cells), in *hOCT2*-expressing cells that were transiently transfected with *LAPTM4A*, as well as in *hOCT2* cells transiently transfected with the control vector pcDNA3.1. In comparison to untransfected cells, transfection with control vehicle did not alter ASP^+ uptake, whereas overexpression of *LAPTM4A* led to a significant reduction of ASP^+ uptake by $23 \pm 3\%$ ($n = 31$) (Fig. 8). To exclude undesirable transfection effects on *hOCT2* expression, and to control transfection efficiency of *LAPTM4A*, real time PCR analysis of the cells was performed after uptake measurements. The results of the real time PCR analysis showed that transfection with either control vector or *LAPTM4A* did not significantly alter *hOCT2* expression on mRNA levels in comparison to untreated cells (Fig. 9). Furthermore,

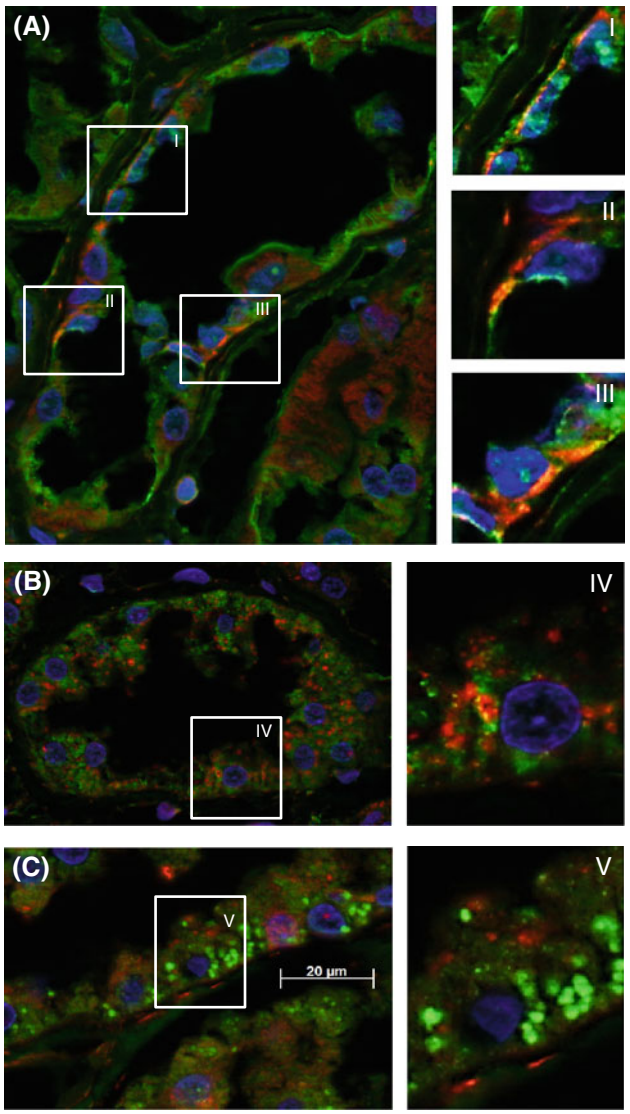

Fig. 7 Immunofluorescence microscopy of human kidneys. Cryosections of human kidneys were immunostained against *LAPTM4A* (*red*) and *hOCT2* (*green*) (**a**), *LAPTM4A* (*green*) and *LAMP1* (*red*) (**b**) and *LAPTM4A* (*red*) and *EEA1* (*green*) (**c**), respectively. Primary antibodies were visualized with Alexa 594 and Star36D 488 secondary antibodies. Partial colocalization (*yellow*) was readily detected between *LAPTM4A* and *hOCT2* (**a**) as well as *LAPTM4A* and LAMP1 (**b**), whereas no significant colocalization was found between *LAPTM4A* and *EEA1* (**c**)

RT-PCR revealed 435-fold overexpression of *LAPTM4A* in *LAPTM4A*-transfected cells compared with untransfected cells.

Effects of *LAPTM4A* on *hOCT2* surface expression

In order to further analyze the effects of *LAPTM4A* on *hOCT2* surface expression, biotinylation experiments were performed. In comparison to control transfection

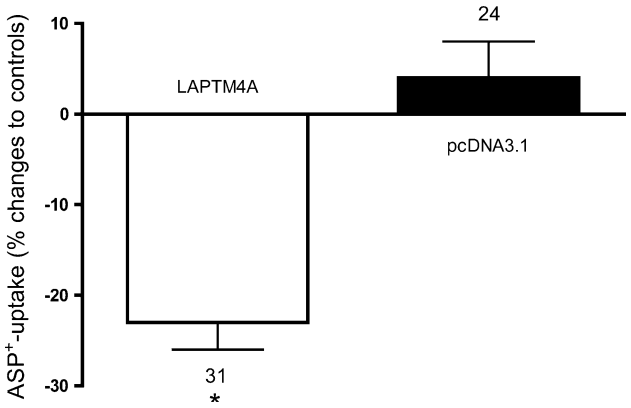

Fig. 8 Regulation of *hOCT2* mediated ASP^+-uptake by overexpression of *LAPTM4A* in HEK293 *hOCT2* stably expressing cells: 48 h after transfection with *LAPTM4A* or pcDNA3.1, ASP^+-uptake was measured as initial fluorescence increase. Initial uptake rates of ASP^+ are presented as % uptake of untransfected controls. The number of experiments is indicated above the columns. Values are mean ± SEM; *statistically significant effects from controls (ANOVA) ($P < 0.05$)

overexpression of *LAPTM4A* led to a significant decrease of *hOCT2* plasma membrane expression ($-60 \pm 17\%$; $n = 3$) (Fig. 10). Furthermore, quantitative analysis of whole cell lysates demonstrated that *LAPTM4A* leads to a diminished overall *hOCT2* expression, thus indicating that *hOCT2* is not only removed from/or not trafficked to plasma membranes but is also further delivered and probably metabolised by the endocytotic machinery (Fig. 11).

Discussion

In this work, we demonstrate that *hOCT2* interacts with *LAPTM4A* in lysosomes and late endosomes and most likely induces endocytotic degradation. This interaction has been first revealed on the protein level using mbSUS and FRET, two approaches using living cells. The mbSUS methodology is a special yeast two-hybrid technique for membrane proteins, where interactions of proteins take place in vivo directly at the plasma membrane. According to the results of this assay, *hOCT2* interacts directly with *LAPTM4A* in the cell membranes. This interaction has been confirmed by FRET analysis, where a significant FRET signal was observed in submembraneous intracellular vesicles. The interaction detected with these two in vivo assays was also confirmed by pulldown experiments. *LAPTM4A* is a four-transmembrane-spanning protein of 27 kDa that has been first described as mouse transporter protein (*MTP*) [26]. The cellular expression of *LAPTM4A* in late endosomes and lysosomes [23] seems to be determined by two tandemly arranged tyrosine-based sorting signals [27]. At tissue level, *LAPTM4A* is ubiquitarily

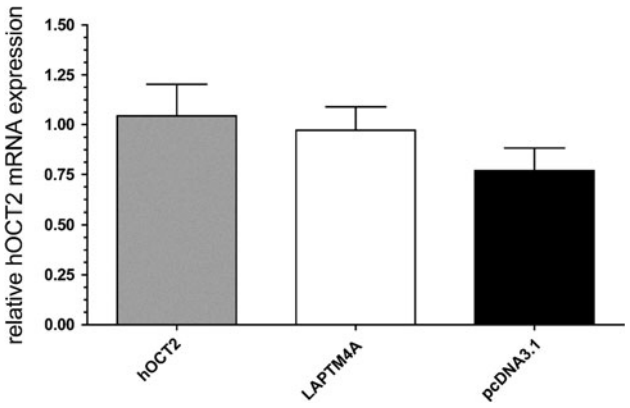

Fig. 9 Real time PCR analysis of *hOCT2* expression in HEK293-*hOCT2* cells either transfected with *LAPTM4A* or pcDNA3.1. Results are expressed as relative *hOCT2* mRNA expression of 5 independent experiments each. *GAPDH* was used as internal standard for normalization. Values are mean ± SEM

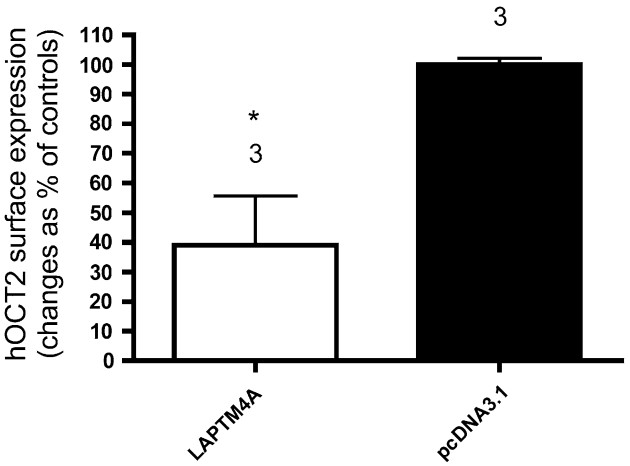

Fig. 10 Effect of *LAPTM4A* overexpression in HEK293-*hOCT2* cells on *hOCT2* plasma membrane expression after quantitative western blot analysis of three independent surface biotinylation experiments. Results are shown as changes in % of controls. The number of experiments is indicated above the columns. *Statistically significant different *hOCT2* expression (unpaired *t* test) ($P < 0.05$)

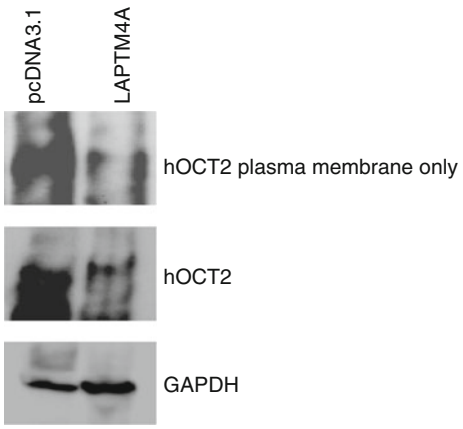

Fig. 11 Representative images of western blot analysis of HEK293-*hOCT2* cells after transfection with either control vehicle (pcDNA3.1) or *LAPTM4A*. Shown are the representative results of 3 identical surface biotinylation experiments, analysis of whole cell lysates and *GAPDH* as loading control

expressed [28]. When expressed in a drug-sensitive strain of the yeast *Saccharomyces cerevisiae, MTP* seems to regulate the subcellular localization and hence the cytotoxicity of several substances [29]. Interestingly, among these substances there are organic cations that are substrates of OCTs. For this reason, two explanations for the biological significance of the interaction *hOCT2-LAPTM4A* can be offered: first, this interaction may give origin to a tandem structure, where organic cations, binding at the plasma membrane to *hOCT2*, are immediately directed by *LAPTM4A* to lysosomes, where they accumulate. Alternatively, the interaction leads to recruitment of OCTs in an endocytotic compartment, where the complex *hOCT2-LAPTM4A* is digested. The second hypothesis seems to be confirmed by surface biotinylation experiments with *hOCT2*-expressing HEK293 cells transfected with *LAPTM4A*: this transfection resulted in a reduction of *hOCT2* expression on the plasma membrane as well as a decrease of the amount of overall cellular *hOCT2*. Moreover, the transfection of *LAPTM4A* in *hOCT2*-expressing HEK293 cells significantly decreased the transport rate of the fluorescent organic cation ASP^+. These two findings strongly speak for a role of *LAPTM4A* in recruiting *hOCT2* to an endocytotic pathway. Nevertheless, it remains unclear if, on the one hand, *LAPTM4A* leads to a direct or indirect trafficking from the plasma membrane to endosomes/lysosomes, or, on the other hand, interaction with *hOCT2* takes place mainly intracellularily and leads to immediate metabolization after synthesis in ER or Golgi apparatus. Furthermore, the mbSUS showed that *LAPTM4A* also interacts directly at cell membranes of yeasts with *hOCT1* and *hOCT3*. Interestingly, both OCT2 and OCT3 play an important role in the dopaminergic brain activity. The endogenous dopaminergic neuromodulators cyclo(his-pro) and salsolinol have been proposed as key substrates of *hOCT2* [12]. Both substrates are abundant in the dopaminergic brain region of the substantia nigra, where OCT2 shows its highest expression in CNS [12]. It is proposed that an intracellular OCT2-mediated balance of salsolinol and cyclo(his-pro) is crucial for maintenance of dopaminergic cell integrity. A rise in potentially cytotoxic salsolinol or a decline in protective cyclo(his-pro) may cause calcium-triggered apoptotic cell death, possibly contributing to the selective chronic nigral degeneration observed in Parkinson's disease [12]. On the other hand, due to its expression in non-dopaminergic cells adjacent to both the soma and terminals of midbrain dopaminergic neurons, OCT3 has also been suggested to contribute to the

dopaminergic damage by bidirectionally regulating the bioavailability of toxic species [30]. These findings underline the potential decisive role of OCT in the development of neurodegenerative diseases. In this view, the interaction of *LAPTM4A* with OCT could be of importance, considering that, in brain of aged dogs, which develop similar neurological features as elderly humans, a significant upregulation of *LAPTM4A*-mRNA expression was found [31]. In the future, the role of the regulation of OCT expression and function by the interaction with *LAPTM4A* should be considered when investigating the role of dopaminergic signalling pathways in neurodegenerative diseases such as Parkinson's and Alzheimer's diseases. Because of the high expression of OCT in excretory organs such as the kidneys (OCT2) and the liver (OCT1), the interaction with *LAPTM4A* may also play an important role in controlling the excretion and the blood concentration of several cationic drugs. OCTs play a crucial role for the uptake of these drugs not only in target but also non-target cells. For example, the expression of OCT1 in myeloid leukemia cells correlates with the antitumoral effectiveness of imatinib [32], a substrate of OCT1, while the expression of OCT2 in the kidneys and in the cochlea seems to be critically involved in the development of the nephrotoxic and ototoxic side effects of tumor therapy with cisplatin [33], a substrate for OCT2. Since proteins of the LAPTM family are overexpressed in many types of cancer, due to the negative correlation of their expression with OCT function, a resistance of tumors against chemotherapy could result. Indeed, the expression of *LAPTM4A* in *Saccharomyces cerevisiae* induced a multidrug-resistant phenotype [29] and the resistance against cisplatin of glioblastoma cells pretreated with hepatocyte growth factor was associated with an increased expression of *LAPTM4A* [34]. Furthermore, McLean et al. [35] demonstrated in a pharmakogenomic analysis that overexpression of *LAPTM4A* is associated with a poorer response of chronic myeloic leucemia patients to the tyrosine kinase-inhibiting drug imatinib, which has been shown to be a substrate for organic cation transporters [36, 37].

In conclusion, we demonstrated that *hOCT2* interacts in vivo with *LAPTM4A* and that this interaction is linked with the entry of *hOCT2* in an endocytotic pathway. Because of the important role played by OCT2 in the brain and renal dopaminergic signaling pathway, and in the desired or undesired drug uptake, and because *LAPTM4A* is upregulated in neurodegenerative diseases and in chemoresistant cells, this interaction has important physiological, pathophysiological, and pharmacological implications. Moreover, a new function of *LAPTM4A*, as recruiting protein for the endocytotic pathway, has been discovered.

Acknowledgments The authors are grateful to Julia Humberg, Rita Schröter, Bernadette Gelschefarth and Ute Neugebauer for excellent technical assistance. This study was supported by the Deutsche Forschungsgemeinschaft (CI 107/4-1).

References

1. Busch AE, Karbach U, Miska D, Gorboulev V, Akhoundova A, Volk C, Arndt P, Ulzheimer JC, Sonders MS, Baumann C, Waldegger S, Lang F, Koepsell H (1998) Human neurons express the polyspecific cation transporter hOCT2, which translocates monoamine neurotransmitters, amantadine, and memantine. Mol Pharmacol 54:342–352
2. Ogasawara M, Yamauchi K, Satoh Y, Yamaji R, Inui K, Jonker JW, Schinkel AH, Maeyama K (2006) Recent advances in molecular pharmacology of the histamine systems: organic cation transporters as a histamine transporter and histamine metabolism. J Pharmacol Sci 101:24–30
3. Urakami Y, Kimura N, Okuda M, Inui K (2004) Creatinine transport by basolateral organic cation transporter hOCT2 in the human kidney. Pharm Res 21:976–981
4. Barendt WM, Wright SH (2002) The human organic cation transporter (hOCT2) recognizes the degree of substrate ionization. J Biol Chem 277:22491–22496
5. Kimura N, Okuda M, Inui K (2005) Metformin transport by renal basolateral organic cation transporter hOCT2. Pharm Res 22:255–259
6. Yonezawa A, Masuda S, Yokoo S, Katsura T, Inui K (2006) Cisplatin and oxaliplatin, but not carboplatin and nedaplatin, are substrates for human organic cation transporters (SLC22A1–3 and multidrug and toxin extrusion family). J Pharmacol Exp Ther 319:879–886
7. Ciarimboli G, Ludwig T, Lang D, Pavenstadt H, Koepsell H, Piechota HJ, Haier J, Jaehde U, Zisowsky J, Schlatter E (2005) Cisplatin nephrotoxicity is critically mediated via the human organic cation transporter 2. Am J Pathol 167:1477–1484
8. Busch AE, Quester S, Ulzheimer JC, Waldegger S, Gorboulev V, Arndt P, Lang F, Koepsell H (1996) Electrogenic properties and substrate specificity of the polyspecific rat cation transporter rOCT1. J Biol Chem 271:32599–32604
9. Gorboulev V, Ulzheimer JC, Akhoundova A, Ulzheimer-Teuber I, Karbach U, Quester S, Baumann C, Lang F, Busch AE, Koepsell H (1997) Cloning and characterization of two human polyspecific organic cation transporters. DNA Cell Biol 16:871–881
10. Ciarimboli G, Schlatter E (2005) Regulation of organic cation transport. Pflugers Arch 449:423–441
11. Ciarimboli G (2008) Organic cation transporters. Xenobiotica 38:936–971
12. Taubert D, Grimberg G, Stenzel W, Schomig E (2007) Identification of the endogenous key substrates of the human organic cation transporter OCT2 and their implication in function of dopaminergic neurons. PLoS One 2:e385
13. Urakami Y, Okuda M, Masuda S, Akazawa M, Saito H, Inui K (2001) Distinct characteristics of organic cation transporters, OCT1 and OCT2, in the basolateral membrane of renal tubules. Pharm Res 18:1528–1534
14. Motohashi H, Sakurai Y, Saito H, Masuda S, Urakami Y, Goto M, Fukatsu A, Ogawa O, Inui KK (2002) Gene expression levels and immunolocalization of organic ion transporters in the human kidney. J Am Soc Nephrol 13:866–874
15. Urakami Y, Okuda M, Saito H, Inui K (2000) Hormonal regulation of organic cation transporter OCT2 expression in rat kidney. FEBS Lett 473:173–176

16. Asaka J, Terada T, Okuda M, Katsura T, Inui K (2006) Androgen receptor is responsible for rat organic cation transporter 2 gene regulation but not for rOCT1 and rOCT3. Pharm Res 23:697–704
17. Cetinkaya I, Ciarimboli G, Yalcinkaya G, Mehrens T, Velic A, Hirsch JR, Gorboulev V, Koepsell H, Schlatter E (2003) Regulation of human organic cation transporter hOCT2 by PKA, PI3 K, and calmodulin-dependent kinases. Am J Physiol Renal Physiol 284:F293–F302
18. Ciarimboli G, Struwe K, Arndt P, Gorboulev V, Koepsell H, Schlatter E, Hirsch JR (2004) Regulation of the human organic cation transporter hOCT1. J Cell Physiol 201:420–428
19. Schlatter E, Mönnich V, Cetinkaya I, Mehrens T, Ciarimboli G, Hirsch JR, Popp C, Koepsell H (2002) The organic cation transporters rOCT1 and hOCT2 are inhibited by cGMP. J Membr Biol 189:237–244
20. Mehrens T, Lelleck S, Cetinkaya I, Knollmann M, Hohage H, Gorboulev V, Boknik P, Koepsell H, Schlatter E (2000) The affinity of the organic cation transporter rOCT1 is increased by protein kinase C-dependent phosphorylation. J Am Soc Nephrol 11:1216–1224
21. Soodvilai S, Chatsudthipong A, Chatsudthipong V (2007) Role of MAPK and PKA in regulation of rbOCT2-mediated renal organic cation transport. Am J Physiol Renal Physiol 293:F21–F27
22. Wilde S, Schlatter E, Koepsell H, Edemir B, Reuter S, Pavenstadt H, Neugebauer U, Schroter R, Brast S, Ciarimboli G (2009) Calmodulin-associated post-translational regulation of rat organic cation transporter 2 in the kidney is gender dependent. Cell Mol Life Sci 66:1729–1740
23. Cabrita MA, Hobman TC, Hogue DL, King KM, Cass CE (1999) Mouse transporter protein, a membrane protein that regulates cellular multidrug resistance, is localized to lysosomes. Cancer Res 59:4890–4897
24. Schmid JA, Scholze P, Kudlacek O, Freissmuth M, Singer EA, Sitte HH (2001) Oligomerization of the human serotonin transporter and of the rat GABA transporter 1 visualized by fluorescence resonance energy transfer microscopy in living cells. J Biol Chem 276:3805–3810
25. Bartholomaus I, Milan-Lobo L, Nicke A, Dutertre S, Hastrup H, Jha A, Gether U, Sitte HH, Betz H, Eulenburg V (2008) Glycine transporter dimers: evidence for occurrence in the plasma membrane. J Biol Chem 283:10978–10991
26. Hogue DL, Ellison MJ, Young JD, Cass CE (1996) Identification of a novel membrane transporter associated with intracellular membranes by phenotypic complementation in the yeast *Saccharomyces cerevisiae*. J Biol Chem 271:9801–9808
27. Hogue DL, Nash C, Ling V, Hobman TC (2002) Lysosome-associated protein transmembrane 4 alpha (LAPTM4 alpha) requires two tandemly arranged tyrosine-based signals for sorting to lysosomes. Biochem J 365:721–730
28. Maeda K, Horikoshi T, Nakashima E, Miyamoto Y, Mabuchi A, Ikegawa S (2005) MATN and LAPTM are parts of larger transcription units produced by intergenic splicing: intergenic splicing may be a common phenomenon. DNA Res 12:365–372
29. Hogue DL, Kerby L, Ling V (1999) A mammalian lysosomal membrane protein confers multidrug resistance upon expression in *Saccharomyces cerevisiae*. J Biol Chem 274:12877–12882
30. Cui M, Aras R, Christian WV, Rappold PM, Hatwar M, Panza J, Jackson-Lewis V, Javitch JA, Ballatori N, Przedborski S, Tieu K (2009) The organic cation transporter-3 is a pivotal modulator of neurodegeneration in the nigrostriatal dopaminergic pathway. Proc Natl Acad Sci USA 106:8043–8048
31. Swanson KS, Vester BM, Apanavicius CJ, Kirby NA, Schook LB (2009) Implications of age and diet on canine cerebral cortex transcription. Neurobiol Aging 30:1314–1326
32. Wang L, Giannoudis A, Lane S, Williamson P, Pirmohamed M, Clark RE (2008) Expression of the uptake drug transporter hOCT1 is an important clinical determinant of the response to imatinib in chronic myeloid leukemia. Clin Pharmacol Ther 83:258–264
33. Ciarimboli G, Deuster D, Knief A, Sperling M, Holtkamp M, Edemir B, Pavenstadt H, Lanvers-Kaminsky C, Am Zehnhoff-Dinnesen A, Schinkel AH, Koepsell H, Jurgens H, Schlatter E (2010) Organic cation transporter 2 mediates cisplatin-induced oto- and nephrotoxicity and is a target for protective interventions. Am J Pathol 176:1169–1180
34. Ma Y, Yuan RQ, Fan S, Hu C, Goldberg ID, Laterra JJ, Rosen EM (2006) Identification of genes that modulate sensitivity of U373MG glioblastoma cells to cis-platinum. Anticancer Drugs 17:733–751
35. McLean LA, Gathmann I, Capdeville R, Polymeropoulos MH, Dressman M (2004) Pharmacogenomic analysis of cytogenetic response in chronic myeloid leukemia patients treated with imatinib. Clin Cancer Res 10:155–165
36. White DL, Saunders VA, Dang P, Engler J, Zannettino AC, Cambareri AC, Quinn SR, Manley PW, Hughes TP (2006) OCT-1-mediated influx is a key determinant of the intracellular uptake of imatinib but not nilotinib (AMN107): reduced OCT-1 activity is the cause of low in vitro sensitivity to imatinib. Blood 108:697–704
37. Thomas J, Wang L, Clark RE, Pirmohamed M (2004) Active transport of imatinib into and out of cells: implications for drug resistance. Blood 104:3739–3745
38. Grefen C, Lalonde S, Obrdlik P (2007) Split-ubiquitin system for identifying protein-protein interactions in membrane and full-length proteins. Curr Protoc Neurosci 41:5.27.1–5.27.41
39. Xia Z, Liu Y (2001) Reliable and global measurement of fluorescence resonance energy transfer using fluorescence microscopes. Biophys J 81:2395–2402
40. Sorkin A, McClure M, Huang F, Carter R (2000) Interaction of EGF receptor and grb2 in living cells visualized by fluorescence resonance energy transfer (FRET) microscopy. Curr Biol 10:1395–1398
41. Feige JN, Sage D, Wahli W, Desvergne B, Gelman L (2005) PixFRET, an imageJ plug-in for FRET calculation that can accommodate variations in spectral bleed-throughs. Microsc Res Tech 68:51–58
42. Sitte HH, Farhan H, Javitch JA (2004) Sodium-dependent neurotransmitter transporters: oligomerization as a determinant of transporter function and trafficking. Mol Interv 4:38–47
43. Pietig G, Mehrens T, Hirsch JR, Cetinkaya I, Piechota H, Schlatter E (2001) Properties and regulation of organic cation transport in freshly isolated human proximal tubules. J Biol Chem 276:33741–33746
44. Livak KJ, Schmittgen TD (2001) Analysis of relative gene expression data using real-time quantitative PCR and the 2[-Delta Delta C(T)] method. Methods 25:402–408